E. Butanovs, S. Vlassov, A. Kuzmin, S. Piskunov, J. Butikova, B. Polyakov,
Fast-response single-nanowire photodetector based on ZnO/WS2 core/shell heterostructures,
ACS Appl. Mater. Interfaces 10 (2018) 13869-13876.

Fast-response single-nanowire photodetector based on ZnO/WS_2 core/shell heterostructures

Edgars Butanovs[†], *Sergei Vlassov*[‡], *Alexei Kuzmin*[†], *Sergei Piskunov*[†], *Jelena Butikova*[†], *Boris Polyakov*[†]*

† Institute of Solid State Physics, University of Latvia, Kengaraga street 8, LV-1063 Riga, Latvia

‡ Institute of Physics, University of Tartu, W. Ostwaldi 1, 50411 Tartu, Estonia

KEYWORDS: core/shell nanowires; 1D/1D heterostructures; Van-der-Waals epitaxy; transitional metal chalcogenides; photodetectors

ABSTRACT

The surface plays an exceptionally important role in nanoscale materials, exerting a strong influence on their properties. Consequently, even a very thin coating can greatly improve optoelectronic properties of nanostructures by modifying the light absorption and spatial distribution of charge carriers. To use these advantages, 1D/1D heterostructures of ZnO/WS_2 core/shell nanowires with a-few-layers thick WS_2 shell were fabricated. These heterostructures were thoroughly characterized by scanning and transmission electron microscopy, X-ray diffraction and Raman spectroscopy. Then, a single-nanowire photoresistive device was assembled by mechanically positioning ZnO/WS_2 core/shell nanowires onto gold electrodes

E. Butanovs, S. Vlassov, A. Kuzmin, S. Piskunov, J. Butikova, B. Polyakov,
Fast-response single-nanowire photodetector based on ZnO/WS2 core/shell heterostructures,
ACS Appl. Mater. Interfaces 10 (2018) 13869-13876.

inside a scanning electron microscope. The results show that a few layers of WS_2 significantly enhance photosensitivity in the short wavelength range and drastically (almost two orders of magnitude) improve the photoresponse time of pure ZnO nanowires. The fast response time of ZnO/WS_2 core/shell nanowire was explained by electrons and holes sinking from ZnO nanowire into WS_2 shell, which serves as a charge carrier channel in ZnO/WS_2 heterostructure. First-principles calculations suggest that the interface layer i-WS_2, bridging ZnO nanowire surface and WS_2 shell, might play a role of energy barrier preventing backward diffusion of charge carriers into ZnO nanowire.

Introduction

Nanostructured photodetectors operating from ultraviolet (UV) to terahertz frequencies have attracted much attention during the last few decades due to their appealing performance for various applications.[1] Such nanodevices made of quantum dots, nanowires, nanobelts, nanotubes or nanolayers demonstrate high integration density and sensitivity, fast response and multifunctionality.[2–5] Current developments in the field are concentrated on precisely controlling the manufacturing of nanostructured materials, modifying their properties and developing methods for mass production.[6]

Photodetectors based on one-dimensional (1D) nanostructured materials have become one of the most attractive photoelectronic devices that can be implemented using individual or assemblies of nanostructures.[4,7] A fabrication of hybrid nanostructures composed of two or more components opens new possibilities to control their properties, in particular, in photodetection capability in a broad spectral range from UV to infrared.[7] Depending on the dimensionality of constituting components, hybrid nanostructures can be classified into six types,[7] and the 1D/1D

E. Butanovs, S. Vlassov, A. Kuzmin, S. Piskunov, J. Butikova, B. Polyakov,
Fast-response single-nanowire photodetector based on ZnO/WS2 core/shell heterostructures,
ACS Appl. Mater. Interfaces 10 (2018) 13869-13876.

nanostructured photodetectors constitute the subject of the present study. Furthermore, they can be realized as core/shell, branched or axial heterojunctions.

Radially heterostructured core/shell nanowires (NWs) are intriguing and prospective types of nanomaterials, and these NWs have been intensively explored recently.[8–10] The surface of NWs plays an important role, because the surface is often the origin of structural and electronic defects. Properly chosen shell material can protect the core and significantly improve its electrical, mechanical and optical properties.[9,11,12] Therefore, the engineering of core/shell heterostructures is a versatile tool for creating novel advanced nanostructures with desired properties.

ZnO NWs are among the most popular nanomaterials with a wide range of applications in nanoelectronics, sensorics and nanophotonics, including the use of ZnO NWs as piezoelectric nanogenerators and ultraviolet (UV) photodetectors.[13,14] At ambient conditions, the most stable phase of ZnO has n-type conductivity and is hexagonal wurtzite-type with a direct band gap about 3.2–3.3 eV.[15] Cubic zinc blend and rock-salt ZnO phases can be also obtained at specific conditions.[15] ZnO NW UV photodetectors demonstrate excellent performance and sensitivity; however, their time response is relatively slow, being in the range of seconds.[16–18] There are several reasons for slow photoresponse of ZnO NW photodetectors, namely surface charge traps and surface states related to adsorbed oxygen molecules.[19] An obvious method to make photodetector faster is to etch and passivate NW surface layer, as it was demonstrated by Mallampati et al.[20] Cheng et al used electric field of Shottky barrier to increase both speed and gain of ZnO NW photodetector.[19] In a number of works significant improvement of ZnO NW photodetectors responsivity and speed was achieved by Au nanoparticles decoration.[21, 22]

E. Butanovs, S. Vlassov, A. Kuzmin, S. Piskunov, J. Butikova, B. Polyakov,
Fast-response single-nanowire photodetector based on ZnO/WS2 core/shell heterostructures,
ACS Appl. Mater. Interfaces 10 (2018) 13869-13876.

Another promising class of nanomaterials consists of layered 2D transition metal dichalcogenides (TMDs), and they have recently attracted much attention.[23,24] For example, several state-of-the-art 1D and 2D WS_2 and MoS_2-based high sensitivity UV and VIS photodetectors was demonstrated in.[6,24,26] In addition, a-few-layers thick TMDs show a transition from indirect to direct band gap behavior. For example, bulk WS_2 is an n-type semiconductor having an indirect band gap $\Delta\varepsilon_{ig}$ = 1.3–1.4 eV, whereas a monolayer has a direct optical band gap $\Delta\varepsilon_{dg}$ = 1.7–1.9 eV and strong optical absorption, being able to absorb 5–10% of incident light.[27-29] Furthermore, epitaxial growth of WS_2 and MoS_2 is possible on sapphire wafers, because the (0001) plane of c-sapphire is hexagonally arranged, matching the crystal lattice of the two sulphides.[30] Recently, the authors have demonstrated that both WS_2 and MoS_2 can be epitaxially grown around ZnO NWs, producing ZnO/WS_2 and ZnO/MoS_2 core/shell nanostructures.[31,32]

Hybrid or composite TMDs materials have recently attracted significant attention.[24] The use of 2D ZnO/WS_2 heterostructures for enhanced UV photodetectors was demonstrated by Lan et al.[33] The heterostructured device was produced by transferring CVD grown WS_2 monolayer onto the surface of polycrystalline ZnO film deposited by dc magnetron sputtering on glass substrate, and, finally, the aluminium electrodes were fabricated by thermal evaporation through a shadow mask.[33] An enhancement by 16 times (in vacuum) of UV light photodetection by ZnO/WS_2 heterostructure was observed relatively to pure ZnO film. However, the photoresponse time was still measured in the range of seconds.[33]

This study demonstrates significantly enhanced photodetection by ZnO NWs coated with a few WS_2 monolayers (ZnO/WS_2 core/shell NWs) and a drastic (almost two orders of magnitude) improvement of photoresponse time compared to that of pure ZnO NWs. Our results show a

E. Butanovs, S. Vlassov, A. Kuzmin, S. Piskunov, J. Butikova, B. Polyakov,
Fast-response single-nanowire photodetector based on ZnO/WS2 core/shell heterostructures,
ACS Appl. Mater. Interfaces 10 (2018) 13869-13876.

potential of combining layered 2D TMDs materials with semiconducting NWs to create new core/shell heterostructures with advanced optoelectronic properties.

Experimental

Synthesis

The synthesis of ZnO/WS_2 core/shell NWs was described in the authors' previous article.[31] In brief, amorphous a-WO_3 shell was deposited over ZnO NWs by reactive dc magnetron sputtering of a metallic tungsten target in mixed Ar/O_2 atmosphere. Then, ZnO/a-WO_3 NW samples were annealed in a quartz tube in a sulphur atmosphere during 0.5 h at 800°C to convert amorphous tungsten trioxide into tungsten sulphide (WS_2). This process was followed by heating for 0.5 h in inert atmosphere to sublimate excess material.

Sample characterization

The phase composition of ZnO/WS_2 NWs was studied by X-ray diffraction (XRD) at room temperature (20 °C) using a θ-θ Bragg-Brentano powder diffractometer PANalytical X'Pert Pro MPD equipped with copper anode X-ray tube (Model PW3373, Cu K_α radiation). Micro-Raman spectroscopy measurements were performed using a confocal microscope with spectrometer Nanofinders-S (SOLAR TII). A diode pumped solid-state (DPSS) Nd:YAG laser (λ = 532 nm, max continuous wave power P = 150 mW) was used as an excitation source. The Raman spectra were recorded using the monochromator with a 520 mm focal length equipped with 600 grooves/mm diffraction grating and the edge filter to eliminate the elastic component. A Peltier-cooled back-thinned CCD camera (ProScan HS-101H) was employed as a detector of Raman spectra. All measurements were performed in backscattering geometry at room temperature (20

E. Butanovs, S. Vlassov, A. Kuzmin, S. Piskunov, J. Butikova, B. Polyakov,
Fast-response single-nanowire photodetector based on ZnO/WS2 core/shell heterostructures,
ACS Appl. Mater. Interfaces 10 (2018) 13869-13876.

°C) through a Nikon CF Plan Apo 100× (NA = 0.95) optical objective. Furthermore, the morphology of NWs was observed by a SEM (Tescan Lyra XM), and the inner structure of ZnO and ZnO/WS_2 NWs was characterized using a TEM (Tecnai GF20, FEI) operated at the accelerating voltage of 180 kV.

Fabrication of photodetectors

To fabricate single-nanowire photodetectors, gold microelectrodes with the gap width of 2 μm were first obtained on an oxidized silicon wafer by the conventional photolithography technique (as shown in Figure 1). Briefly, the microelectrode pattern was obtained using direct write laser lithography (μPG 101, Heidelberg Instruments) on SU-8 2003 photoresist (MicroChem), and 5/45 nm Cr/Au film was deposited via thermal evaporation method, followed by a lift-off procedure.

Next, single NW photoresistors were fabricated using in situ nanomanipulations inside SEM-FIB Tescan Lyra XM. As-grown ZnO/WS_2 NWs were mechanically transferred from the Si substrate to the as-prepared gold microelectrodes by welding a single NW to the tungsten (W) nanomanipulator probe using electron-beam-assisted platinum (Pt) deposition. Finally, the NW was aligned and placed on top of the microelectrodes, following its cutting off from the W probe with gallium (Ga) ion beam and welding to the electrodes using Pt deposition to ensure the electric contact and fixed position. A SEM image of a typical as-prepared photoresistor is shown in Figure 1c, where the narrow dark strip is the gap between the electrodes, two small rectangles on the NW are the deposited Pt contacts, and the trench is visible at where the NW was cut by the ion beam.

E. Butanovs, S. Vlassov, A. Kuzmin, S. Piskunov, J. Butikova, B. Polyakov,
Fast-response single-nanowire photodetector based on ZnO/WS2 core/shell heterostructures,
ACS Appl. Mater. Interfaces 10 (2018) 13869-13876.

For comparison, WS_2 water suspension was prepared using ultrasound exfoliation of WS_2 powder (Sigma Aldrich). A small amount (36 mg) of WS_2 powder in 6 ml of pure deionized water was ultrasonically processed at 100 W for 3 h. After one day, water suspension of WS_2 was centrifuged and re-suspended in 1 ml tube. A droplet of WS_2 suspension was cast on gold electrodes and heated at 150 °C during 5 min.

Device measurements

Current-voltage (*I-V*) characteristics and photoresponse of the fabricated single-NW photodetectors were measured with a two-contact micro probe station connected to Model 6485 Keithley Picoammeter, Model 2000 Keithley multimeter and a voltage source (33220A Waveform Generator, Agilent). Semiconductor diode lasers with the wavelengths of 405, 532 and 660 nm and the power of 2 W/cm^2 were used as illumination sources for the photoresponse measurements. Optical beam shutter Thorlabs SH05 was employed for time-resolved measurements, and all measurements were performed at room temperature in air.

Computational Details

In this study, hybrid density functional theory (DFT) calculations have been performed using the CRYSTAL computer code,[34] and the code utilizes localized Gaussian type functions (GTFs) in the form of a basis set (BS) centred on atomic nuclei to expand the crystalline orbitals as linear combinations of atomic orbitals (CO LCAO). Fully relaxed ZnO/WS_2 2D interfaces were calculated by means of hybrid exchange correlation functional PBE0 according to the derivations by Perdew et al. and Adamo and Barone.[35,36] For oxygen atoms, the all-valence BSs of atomic GTFs (constructed using pure s- and hybrid sp-AOs) in the form of 8s-411sp were used, and for zinc atoms, the all-valence BS in the form 8s-64111sp-41d were used. In addition, the BS

E. Butanovs, S. Vlassov, A. Kuzmin, S. Piskunov, J. Butikova, B. Polyakov,
Fast-response single-nanowire photodetector based on ZnO/WS2 core/shell heterostructures,
ACS Appl. Mater. Interfaces 10 (2018) 13869-13876.

adopted for sulphur atoms had the form of ECP-1111s-1111p-11d,[33] while for tungsten atoms, the BS that had the form of ECP-11sp-31d56 was used, where ECP represents the effective core pseudopotentials employed to accelerate computation. To provide a balanced summation in both direct and reciprocal lattices, the reciprocal space integration was performed by sampling the interface Brillouin zone (BZ) with the 12 × 12 × 1 Monkhorst−Pack mesh[38] that gives in total 16 k-points evenly distributed at the BZ. Calculations were considered as converged only when the total energy differs by less than 10^{-9} au in two successive cycles of the self-consistent field procedure.

Results and discussion

The phase composition of as-prepared ZnO/WS_2 core/shell NWs on the silicon substrate was studied by X-ray diffraction using the Rietveld method and implemented in the PROFEX code.[39] The result of the Rietveld refinement is shown in Figure 2a. Four crystalline phases corresponding to the Si substrate, ZnO NWs, WS_2 shell and ZnS were detected. While an amount of ZnS on the substrate was high enough to be detected in XRD measurements, only a submonolayer was present inside the ZnO/WS_2 core/shell nanowires.[31]

For room-temperature micro-Raman measurements, the NWs were transferred onto a clean silicon substrate. The Raman spectrum and confocal image (see the inset) of typical individual ZnO/WS_2 core/shell NW are shown in Figure 2b. Two main bands at 354 cm^{-1} and 419 cm^{-1} were detected and attributed to the WS_2 phase. In contrast, no Raman signal from the ZnO NW core was observed because of its very weak intensity when excited at 532 nm. The Raman spectrum of bulk WS_2 measured in a backscattering geometry includes the first-order modes at the centre of the Brillouin zone [in-plane $E^1_{2g}(\Gamma) \approx 355$ cm^{-1} and out-of-plane $A_{1g}(\Gamma) \approx 420$ cm^{-1}],

E. Butanovs, S. Vlassov, A. Kuzmin, S. Piskunov, J. Butikova, B. Polyakov,
Fast-response single-nanowire photodetector based on ZnO/WS2 core/shell heterostructures,
ACS Appl. Mater. Interfaces 10 (2018) 13869-13876.

a zone-edge longitudinal acoustic mode LA(M) ≈ 350 cm^{-1}, and several multi-phonon combinations of these modes.[40-42] When the thickness of WS_2 was reduced to a monolayer, the resonant Raman scattering occurs under 532 nm excitation, enhancing the second-order effects significantly, and the spectrum became very rich in the region of LA(M)-$E^1_{2g}(\Gamma)$ modes.[41,43] In this case, the intensity of the strongest second-order Raman peak, 2LA(M) mode at 354 cm^{-1} (Figure 2b), became dominant, and it overlaps strongly with the first-order $E^1_{2g}(\Gamma)$ mode. Thus, the intensity ratio between 354 cm^{-1} and 419 cm^{-1} bands in the Raman spectrum of the ZnO/WS_2 core/shell NW implies the thickness of the WS_2 shell to be on the order of a monolayer.

The TEM images of pure ZnO NW, ZnO/WS_2 core/shell NW after annealing for 0.5 h in a sulphur atmosphere and after additional annealing in inert atmosphere are shown in Figure 3. Pure ZnO NWs have a smooth surface and a single-crystalline structure (Figure 3b). After annealing in a sulphur atmosphere, many WS_2 layers and protruding WS_2 microplates can be seen on the surface of the NW (Figure 3c,d). However, after annealing in an inert atmosphere, only a few layers of WS_2 remain in agreement with the results of Raman spectroscopy (Figure 2b): the layers appear as black lines parallel to ZnO NW surface (Figure 3e,f). A more detailed description of the TEM investigation of ZnO/WS_2 core/shell NWs and related theoretical models have been published by the authors' previously.[31]

Figure 4 shows measured current-voltage characteristics of photodetectors built using pure ZnO and ZnO/WS_2 core/shell NWs, as well as pure WS_2 flakes. At least five photodetectors of each material were fabricated and measured. The ZnO photoresistor demonstrates a non-symmetric current-voltage $I(V)$ curve (Figure 4a), and this is typical for the Schottky barrier of

E. Butanovs, S. Vlassov, A. Kuzmin, S. Piskunov, J. Butikova, B. Polyakov,
Fast-response single-nanowire photodetector based on ZnO/WS2 core/shell heterostructures,
ACS Appl. Mater. Interfaces 10 (2018) 13869-13876.

ZnO NWs on gold contacts.[44] At the same time, a nearly symmetric response was obtained for WS_2 flakes and ZnO/WS_2 devices (Figure 4b,c).

On-off photoresponse measurements were performed at the bias voltage of 1 V, laser wavelengths of 405, 532 and 660 nm and laser power of 0.5 W/cm^2. Typical photoresponse measurements of pure ZnO and ZnO/WS_2 core/shell NWs and WS_2 flakes-based devices are shown in Figure 5. Pure ZnO NWs respond only to the illumination at a wavelength of 405 nm and do not respond to wavelengths of 532 and 660 nm (Figure 5a). In addition, the photoresponse of WS_2 flakes is almost identical at wavelengths of 405, 532 and 660 nm (Figure 5b). In particular, the photoresponses of ZnO/WS_2 core/shell NWs at 532 and 660 nm are similar, while the photoresponse is significantly stronger at 405 nm (Figure 5c). Since pure ZnO NWs do not respond to green 532 nm (2.33 eV) and red 660 nm (1.88 eV) light because of their wide band gap (E_g = 3.2–3.3 eV), the photoresponse of ZnO/WS_2 core/shell NWs to red and green light is caused by the WS_2 shell. For violet light (405 nm), both ZnO core and WS_2 shell contribute proportionally to the photoresponse of ZnO/WS_2 core/shell NWs.

Time-resolved photoresponse measurements are presented in Figure 5d-f, and the corresponding data are given in Table 1. A slow response of pure ZnO NWs on the timescale of seconds is typical for this material.[16–18] The photoresponse time of WS_2 flake devices is significantly faster than that of ZnO based devices: it depends on the material fabrication method and the number of WS_2 layers.[45,46] Perea-López et al. reported the response time of a few layer WS_2 photodetector as fast as 5.3 ms,[45] while Huo et al. reported the response time of a multilayer WS_2 photodetector to be faster than 20 ms.[46] The time response of the proposed 1D ZnO/WS_2 core/shell NWs is significantly faster than that of 2D ZnO/WS_2-based heterostructured thin film devices.[33] We believe that the faster response time of 1D ZnO/WS_2 NWs in comparison to 2D

E. Butanovs, S. Vlassov, A. Kuzmin, S. Piskunov, J. Butikova, B. Polyakov,
Fast-response single-nanowire photodetector based on ZnO/WS2 core/shell heterostructures,
ACS Appl. Mater. Interfaces 10 (2018) 13869-13876.

heterostructures can be explained by a good quality of ZnO-WS_2 interface (perfect match and close contact between WS_2 and ZnO) which allows fast transfer of photogenerated charge carriers from ZnO to WS_2. The quality of the interface is achieved by direct growth of WS_2 layer on ZnO nanowire surface.

The influence of oxygen molecules on surface states of ZnO NW and their effect on photoresponse kinetics was widely discussed in the literature.[19,20] The presence of WS_2 shell protects ZnO surface from oxygen adsorption and might influence surface related photoinduced processes. Moreover, WS_2 shell might passivate ZnO surface leading to a decrease of charge carrier trapping centers in ZnO NW and be responsible for faster photodetector kinetics. A comparison of the positions of valence and conduction bands of ZnO and WS_2 shows that both electrons and holes should sink into the WS_2 shell[31] and serve as a charge carrier channel in ZnO/WS_2 heterostructure (Figure 6). This conclusion is supported by electronic density of states (DOS) calculated for the ZnO/WS_2 interface layer by means of density functional theory (Figure 6c–e). The DOS calculated for pristine n-type ZnO (1–100) surface of the bare ZnO NW yields a band gap of 3.36 eV (Figure 6c) in good agreement with the experimental observation (3.3 eV [15]). The doping of the surface of NWs with sulphur is the initial stage of ZnO/WS_2 interface formation.[31] The surface of NWs doped with sulphur has a narrower band gap of 1.42 eV due to the presence of occupied in-gap sulphur levels located at 1–2 eV above the top of the valence band of pristine ZnO (1–100), as shown in Figure 6d. The formation of a net of WS_2 bridges as precursors for complete interface formation[31] makes the band gap even more narrow at 1.14 eV (Figure 6e) due to the presence of a sharp peak containing an admixture of W and S states at the top of the valence band. Therefore, according to DFT calculations the interface layer i-WS_2,

E. Butanovs, S. Vlassov, A. Kuzmin, S. Piskunov, J. Butikova, B. Polyakov,
Fast-response single-nanowire photodetector based on ZnO/WS2 core/shell heterostructures,
ACS Appl. Mater. Interfaces 10 (2018) 13869-13876.

bridging ZnO surface and WS_2 shell, has even more narrow gap than WS_2 itself, leading to a formation of energy barrier able to prevent backward diffusion of charge carriers into ZnO NW.

To evaluate the parameters of photoconducting materials, spectral responsivity R_λ and external quantum efficiency *EQE* were calculated according to the following formulas[6,25,26] $R_\lambda = I_\lambda / P_\lambda S$; where I_λ represents the photocurrent, P_λ represents the light intensity and S represents the effective illuminated area; and $EQE = hcR_\lambda / e\lambda$ where h represents Planck's constant, c represents the velocity of light, e represents the charge of electron and λ represents wavelength. In addition, a higher R_λ and *EQE* corresponds to a higher light sensitivity of a material. The calculated values of R_λ and *EQE* for our photodetectors are given in Table 2, and the obtained data are comparable to other state-of-the-art ZnO nanowire- and WS_2 nanotube-based photodetectors. For example, Guo et al. demonstrated the high responsivity of a ZnO nanowire-based UV photodetector having 40 A/W; however, at 10 V, the kinetics of the photodetector was measured in the range of seconds.[17] In contrast, Zhang et al. demonstrated a multiwall WS_2 nanotube-based photodetector with R_λ = 3.14 A/W (at 0.5 V) and *EQE* = 615% for 633 nm light.[26]

Finally, ZnO/WS_2 core/shell NWs with a few WS_2 layers thickness is considered as a WS_2 nanotube wrapped around ZnO NW core. However, such WS_2 nanotubes with the same diameter collapse without an inner ZnO core, because the ZnO core can be etched away in template-assisted synthesis methods.[47,48] Therefore, 1D/1D ZnO/WS_2 core/shell NWs were considered as a convenient object (where ZnO may be a sacrificial template if necessary[49] to manipulate a few-layers thick 2D materials (WS_2, MoS_2 and others), and similar materials can be useful in nanoelectronic and optoelectronic devices.

E. Butanovs, S. Vlassov, A. Kuzmin, S. Piskunov, J. Butikova, B. Polyakov,
Fast-response single-nanowire photodetector based on ZnO/WS2 core/shell heterostructures,
ACS Appl. Mater. Interfaces 10 (2018) 13869-13876.

Conclusions

In summary, an effective photodetector based on ZnO/WS_2 core/shell nanowire (with a few layers of WS_2) is demonstrated in this work. The photodetector responds to illumination at wavelengths of 660 nm (R_λ=1.75), 532 nm (R_λ=2.25) and 405 nm (R_λ=7). The ZnO/WS_2 core/shell nanowire-based device shows clear advantage over pure ZnO nanowire-based photodetector in both higher responsivity (4.6 fold) and faster operation (90 fold) for 405 nm illumination. The photodetector band diagram was supported by first-principles calculations, suggesting that the interface layer i-WS_2, bridging ZnO nanowire surface and WS_2 shell, might play an important role in preventing backward diffusion of charge carriers into ZnO nanowire, whereas WS_2 shell serves as a charge carrier channel in ZnO/WS_2 heterostructure. The obtained results clearly show the potential of combining layered 2D TMDs materials with semiconducting nanowires to create novel core/shell heterostructures with advanced optoelectronic properties.

E. Butanovs, S. Vlassov, A. Kuzmin, S. Piskunov, J. Butikova, B. Polyakov,
Fast-response single-nanowire photodetector based on ZnO/WS2 core/shell heterostructures,
ACS Appl. Mater. Interfaces 10 (2018) 13869-13876.

FIGURES

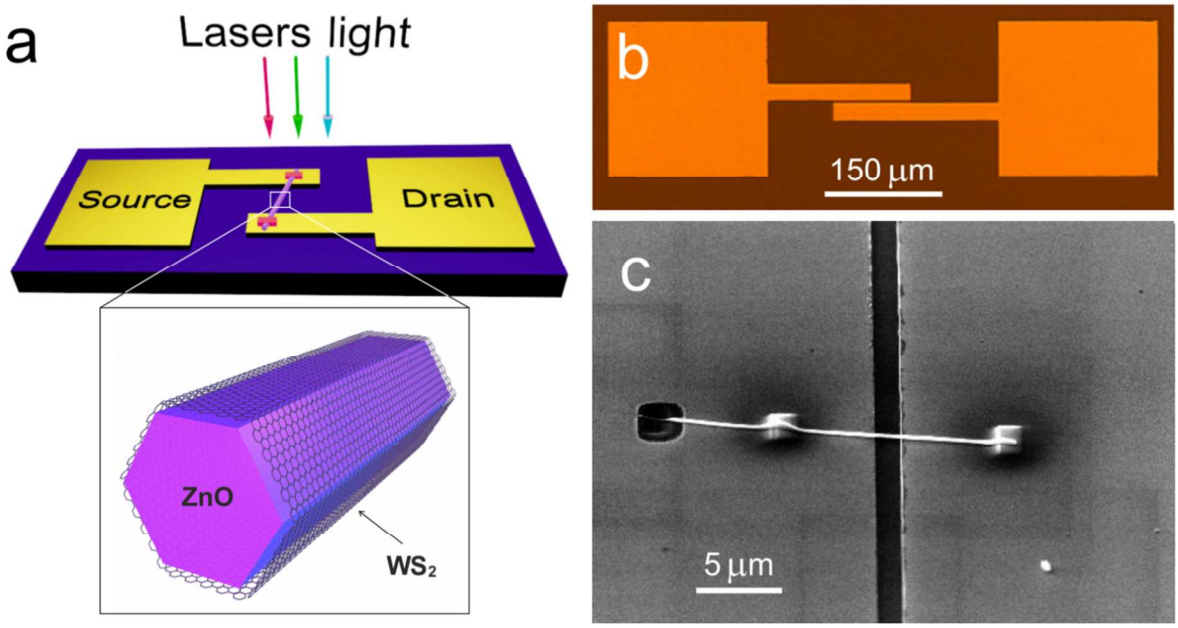

Figure 1. Schematics of ZnO/WS_2 core/shell nanowire-based photodetector (a). Optical microscope image of gold microelectrodes on the oxidized silicon substrate (b). SEM images of a typical nanowire photoresistor (c).

E. Butanovs, S. Vlassov, A. Kuzmin, S. Piskunov, J. Butikova, B. Polyakov,
Fast-response single-nanowire photodetector based on ZnO/WS2 core/shell heterostructures,
ACS Appl. Mater. Interfaces 10 (2018) 13869-13876.

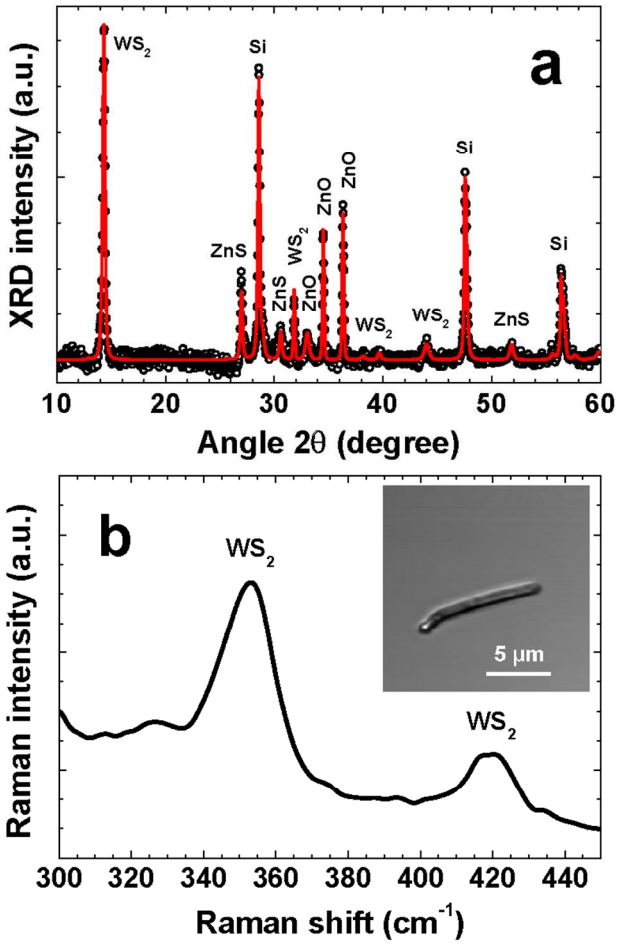

Figure 2. Rietveld refinement (solid line) of the X-ray diffraction pattern (open circles) of the ZnO/WS_2 sample (a). Raman spectrum of the ZnO/WS_2 core/shell nanowire (Inset: confocal microscope image of the nanowire) (b).

E. Butanovs, S. Vlassov, A. Kuzmin, S. Piskunov, J. Butikova, B. Polyakov,
Fast-response single-nanowire photodetector based on ZnO/WS2 core/shell heterostructures,
ACS Appl. Mater. Interfaces 10 (2018) 13869-13876.

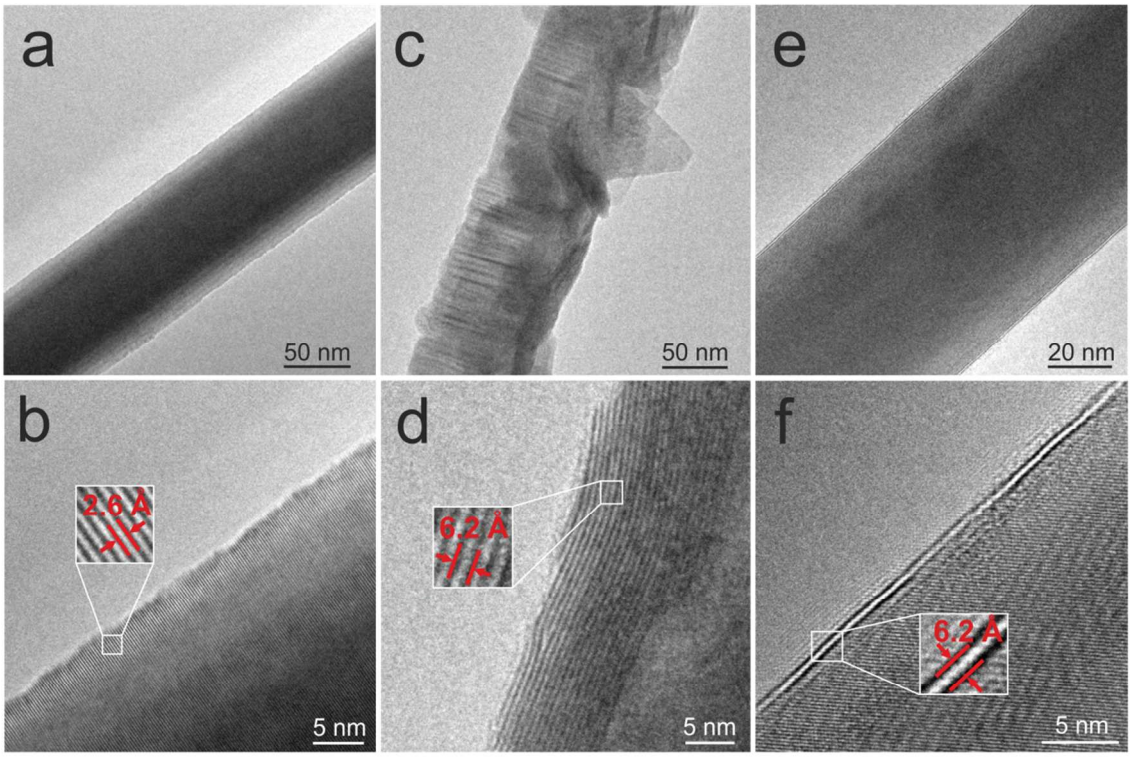

Figure 3. TEM images of pure ZnO nanowire (a, b), ZnO/WS_2 nanowire annealed in sulphur atmosphere (c, d) and ZnO/WS_2 nanowire additionally annealed in inert atmosphere (e, f).

E. Butanovs, S. Vlassov, A. Kuzmin, S. Piskunov, J. Butikova, B. Polyakov,
Fast-response single-nanowire photodetector based on ZnO/WS2 core/shell heterostructures,
ACS Appl. Mater. Interfaces 10 (2018) 13869-13876.

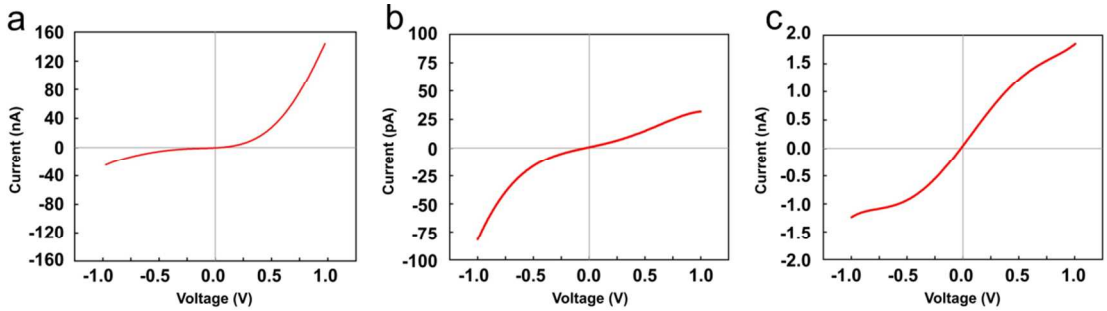

Figure 4. *I-V* characteristics of pure ZnO NW (a), WS_2 flakes drop-cast on electrodes (b), annealed ZnO/WS_2 NW (c).

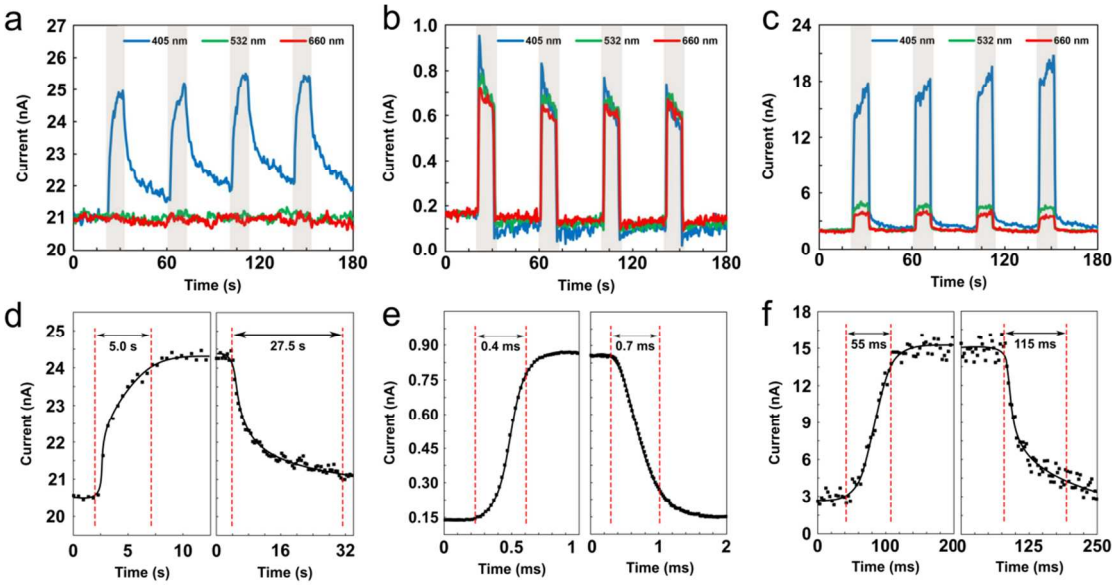

Figure 5. On-off photoresponse measurements of ZnO nanowire (a), WS_2 flakes (b), ZnO/WS_2 nanowire (c) photoresistors at 1V bias voltage and light illumination using 0.5 W/cm^2 light intensity of 405 nm, 532 nm and 660 nm wavelengths. Time-resolved photoresponse measurements of ZnO nanowire (d), WS_2 flakes (e), ZnO/WS_2 nanowire (f) photoresistors at 1V bias voltage and light illumination using 0.5 W/cm^2 intensity of at 405 nm, 532 nm and 660 nm wavelengths.

E. Butanovs, S. Vlassov, A. Kuzmin, S. Piskunov, J. Butikova, B. Polyakov,
Fast-response single-nanowire photodetector based on ZnO/WS2 core/shell heterostructures,
ACS Appl. Mater. Interfaces 10 (2018) 13869-13876.

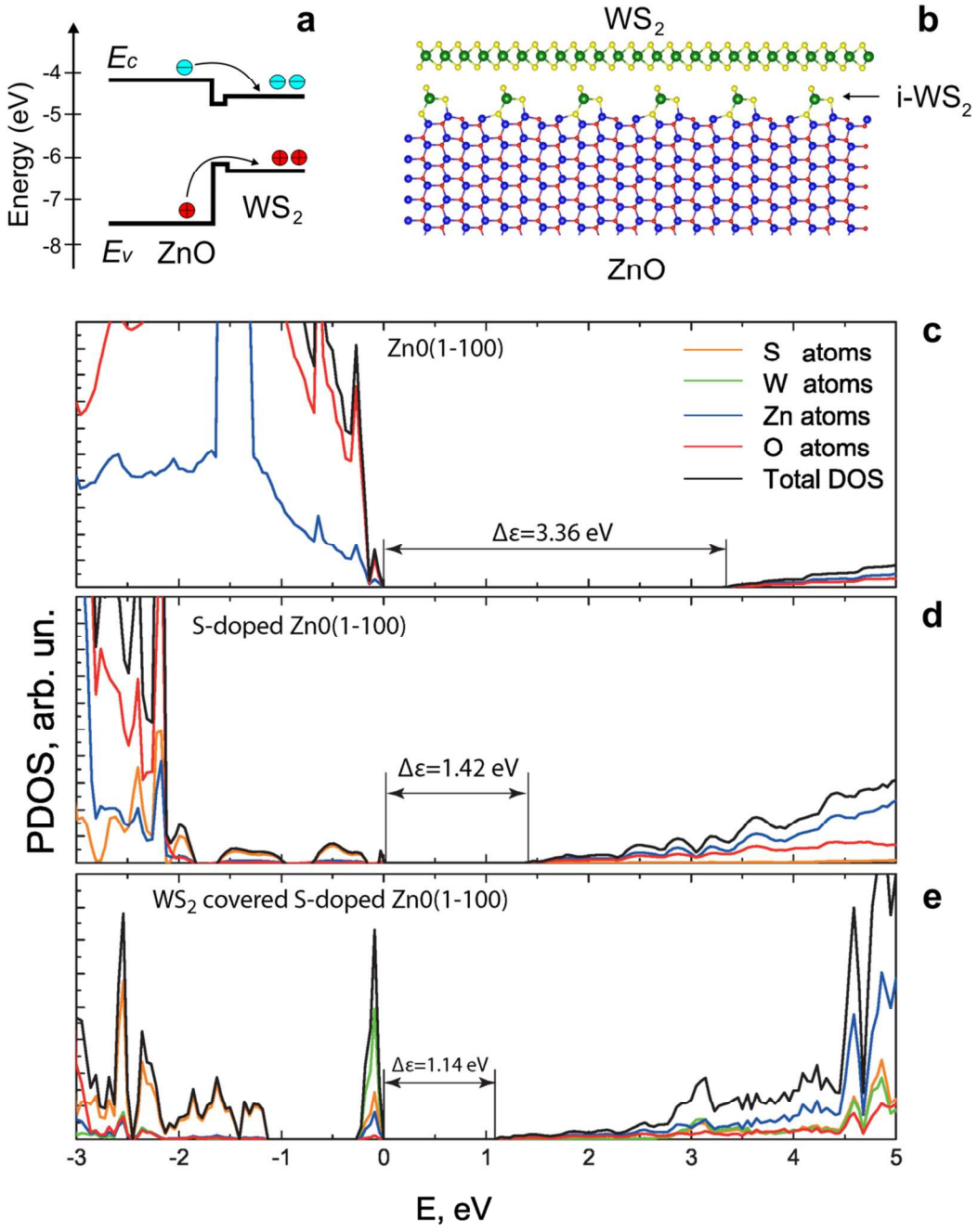

Figure 6. Simplified band diagram of the ZnO-WS_2 core-shell NW (a). Atomic structure of ZnO-WS_2 interface (b). Total and projected densities of states (DOS) of (c) n-type ZnO (1–100) substrate, (d) S-doped ZnO (1–100) substrate, and (e) WS_2 covered S-doped ZnO (1–100) substrate as calculated by means of density functional theory. Zero energy corresponds to the top of the valence band.

E. Butanovs, S. Vlassov, A. Kuzmin, S. Piskunov, J. Butikova, B. Polyakov,
Fast-response single-nanowire photodetector based on ZnO/WS2 core/shell heterostructures,
ACS Appl. Mater. Interfaces 10 (2018) 13869-13876.

TABLES

Table 1. Photoresponse (rise and decay) time of photodetectors fabricated from pure ZnO and ZnO/WS_2 core/shell NWs as well as WS_2 flakes.

Wavelength (nm)	ZnO NWs		WS_2 flakes		ZnO/WS_2 NWs	
	Rise (s)	Decay (s)	Rise (ms)	Decay (ms)	Rise (ms)	Decay (ms)
405	5	27.5	0.4	0.7	55	115
532	-	-	0.3	0.65	21	95
660	-	-	0.53	1.35	22	50

Table 2. Characteristic parameters of photodetectors fabricated from pure ZnO and ZnO/WS_2 core/shell NWs as well as WS_2 flakes.

Parameter	Wavelength (nm)	ZnO NWs	WS_2 flakes	ZnO/WS_2 core/shell NWs
Responsivity or R_λ (A/W)	405	1.50	5.03×10^{-4}	7.00
	532	-	4.84×10^{-4}	2.25
	660	-	4.58×10^{-4}	1.75
EQE (%)	405	4.59	1.5×10^{-3}	21.4
	532	-	1.1×10^{-3}	5.2
	660	-	8.6×10^{-4}	3.3

E. Butanovs, S. Vlassov, A. Kuzmin, S. Piskunov, J. Butikova, B. Polyakov,
Fast-response single-nanowire photodetector based on ZnO/WS2 core/shell heterostructures,
ACS Appl. Mater. Interfaces 10 (2018) 13869-13876.

ASSOCIATED CONTENT

Supporting Information

On-Off photoresponse graphs for selected ZnO-WS_2 and ZnO based photodetector devices (PDF). The following file is available free of charge.

AUTHOR INFORMATION

Corresponding Author

Boris Polyakov, e-mail: boris@cfi.lu.lv

Institute of Solid State Physics, University of Latvia, Kengaraga street 8, LV-1063 Riga, Latvia.

Author Contributions

The manuscript was written through contributions of all authors. All authors have given approval to the final version of the manuscript.

NOTES

The authors declare no competing financial interest.

ACKNOWLEDGMENT

This work was supported by the Latvian National Research Program IMIS2 and ISSP project for Students and Young Researchers Nr. SJZ/2016/6. S.P. is grateful to the ERA.Net RUS Plus WATERSPLIT project no. 237 for the financial support. S.V. is grateful for partial support by the Estonian Science Foundation grant PUT1689.

ABBREVIATIONS

1D one-dimensional; 2D two-dimensional; NW nanowire; TMD transitional metal dichalcogenide; CVD chemical vapour deposition; SEM scanning electron microscope; TEM

E. Butanovs, S. Vlassov, A. Kuzmin, S. Piskunov, J. Butikova, B. Polyakov,
Fast-response single-nanowire photodetector based on ZnO/WS2 core/shell heterostructures,
ACS Appl. Mater. Interfaces 10 (2018) 13869-13876.

transmission electron microscope; XRD X-ray diffraction; DFT density functional theory; EQE external quantum efficiency.

REFERENCES

(1) Chen, H.; Liu, H.; Zhang, Z.; Hu, K.; Fang, X. Nanostructured photodetectors: from ultraviolet to terahertz. *Adv. Mater.* **2016**, *28*, 403–433.

(2) Sang, L.; Liao, M.; Sumiya, M. A comprehensive review of semiconductor ultraviolet photodetectors: from thin film to one-dimensional nanostructures. *Sensors* **2013**, *13*, 10482–10518.

(3) Koppens, F. H. L.; Mueller, T.; Avouris, P.; Ferrari, A. C.; Vitiello, M. S.; Polini, M. Photodetectors based on graphene, other two-dimensional materials and hybrid systems. *Nat. Nanotechnol.* **2014**, *9*, 780.

(4) Chen, H.; Liu, K.; Hu, L.; Al-Ghamdi, A. A.; Fang, X. New concept ultraviolet photodetectors. *Mater. Today* **2015**, *18*, 493–502.

(5) Dhanabalan, S. C.; Ponraj, J. S.; Zhang, H.; Bao, Q. Present perspectives of broadband photodetectors based on nanobelts, nanoribbons, nanosheets and the emerging 2D materials. *Nanoscale* **2016**, *8*, 6410–6434.

(6) Xie, C.; Mak, C.; Tao, X.; Yan, F. Photodetectors based on two-dimensional layered materials beyond graphene. *Adv. Funct. Mater.* **2017**, *27*, 1603886.

(7) Tian, W.; Liu, D.; Cao, F.; Li, L. Hybrid nanostructures for photodetectors. *Adv. Opt. Mater.* **2017**, *5*, 1600468.

(8) Li, Y.; Qian, F.; Xiang, J.; Lieber, C. M. Nanowire electronic and optoelectronic devices. *Mater. Today* **2006**, *9*, 18–27.

(9) Yan, R.; Gargas, D.; Yang, P. Nanowire photonics. *Nat. Photonics* **2009**, *3*, 569.

(10) Kempa, T. J.; Day, R. W.; Kim, S.-K.; Park, H.-G.; Lieber, C. M. Semiconductor nanowires: a platform for exploring limits and concepts for nano-enabled solar cells. *Energy Environ. Sci.* **2013**, *6*, 719–733.

(11) Lauhon, L. J.; Gudiksen, M. S.; Wang, D.; Lieber, C. M. Epitaxial Core–shell and core–multishell nanowire heterostructures. *Nature* **2002**, *420*, 57.

(12) Vlassov, S.; Polyakov, B.; Dorogin, L. M.; Vahtrus, M.; Mets, M.; Antsov, M.; Saar, R.; Romanov, A. E.; Lõhmus, A.; Lõhmus, R. Shape restoration effect in Ag–SiO_2 core–shell nanowires. *Nano Lett.* **2014**, *14*, 5201–5205.

(13) Zhang, Y.; Ram, M. K.; Stefanakos, E. K.; Goswami, D. Y. Synthesis, Characterization, and applications of ZnO nanowires. *J. Nanomater.* **2012**, *2012*, 1–22.

(14) Wang, Z. L. ZnO nanowire and nanobelt platform for nanotechnology. *Mater. Sci. Eng. R Rep.* **2009**, *64*, 33–71.

(15) Özgür, Ü.; Alivov, Y. I.; Liu, C.; Teke, A.; Reshchikov, M. A.; Doğan, S.; Avrutin, V.; Cho, S.-J.; Morkoç, H. A Comprehensive review of ZnO materials and devices. *J. Appl. Phys.* **2005**, *98*, 041301.

(16) Soci, C.; Zhang, A.; Xiang, B.; Dayeh, S. A.; Aplin, D. P. R.; Park, J.; Bao, X. Y.; Lo, Y. H.; Wang, D. ZnO nanowire UV photodetectors with high internal gain. *Nano Lett.* **2007**, *7*, 1003–1009.

(17) Guo, L.; Zhang, H.; Zhao, D.; Li, B.; Zhang, Z.; Jiang, M.; Shen, D. High responsivity ZnO nanowires based UV detector fabricated by the dielectrophoresis method. *Sens. Actuators B Chem.* **2012**, *166–167* (Supplement C), 12–16.

(18) Ates, E. S.; Kucukyildiz, S.; Unalan, H. E. Zinc oxide nanowire photodetectors with single-walled carbon nanotube thin-film electrodes. *ACS Appl. Mater. Interfaces* **2012**, *4*, 5142–5146.

(19) Cheng, G.; Wu, X.; Liu, B; Li, B., Zhang, X.; Du Z. ZnO nanowire Schottky barrier ultraviolet photodetector with high sensitivity and fast recovery speed. *Appl. Phys. Lett.* **2011**, *99*, 203105.

(20) Mallampati, B.; Nair, S. V.; Ruda H.E.; Philipose, U. Role of surface in high photoconductive gain measured in ZnO nanowire-based photodetector. *J. Nanopart. Res.* **2015,** *17*, 176.

(21) Ghimire, R. R.; Nath R.; Neogy R. K.; Raychaudhuri A. K. Ligand-free attachment of plasmonic Au nanoparticles on ZnO nanowire to make a high-performance broadband photodetector using a laser-based method. *Nanotechnology* **2017**, *28*, 295703.

(22) Liu, K.; Sakurai, M.; Liao, M.; Aono, M. Giant improvement of the performance of ZnO nanowire photodetectors by Au nanoparticles. *J. Phys. Chem. C* **2010**, *114*, 19835–19839.

(23) Choi, W.; Choudhary, N.; Han, G. H.; Park, J.; Akinwande, D.; Lee, Y. H. Recent development of two-dimensional transition metal dichalcogenides and their applications. *Mater. Today* **2017**, *20*, 116–130.

(24) Duan, X.; Wang, C.; Pan, A.; Yu, R.; Duan, X. Two-dimensional transition metal dichalcogenides as atomically thin semiconductors: opportunities and challenges. *Chem. Soc. Rev.* **2015**, *44*, 8859–8876.

(25) Zeng, L.; Tao, L.; Tang, C.; Zhou, B.; Long, H.; Chai, Y.; Lau, S. P.; Tsang, Y. H. High-responsivity UV-Vis photodetector based on transferable WS_2 film deposited by magnetron sputtering. *Sci. Rep.* **2016**, *6*, 20343.

(26) Zhang, C.; Wang, S.; Yang, L.; Liu, Y.; Xu, T.; Ning, Z.; Zak, A.; Zhang, Z.; Tenne, R.; Chen, Q. High-performance photodetectors for visible and near-infrared lights based on individual WS_2 nanotubes. *Appl. Phys. Lett.* **2012**, *100*, 243101.

(27) Kam, K. K.; Parkinson, B. A. Detailed photocurrent spectroscopy of the semiconducting Group VIB transition metal dichalcogenides. *J. Phys. Chem.* **1982**, *86*, 463–467.

(28) Kuc, A.; Zibouche, N.; Heine, T. influence of quantum confinement on the electronic structure of the transition metal sulfide TS_2. *Phys. Rev. B* **2011**, *83*, 245213.

(29) Braga, D.; Gutiérrez Lezama, I.; Berger, H.; Morpurgo, A. F. Quantitative determination of the band gap of WS_2 with ambipolar ionic liquid-gated transistors. *Nano Lett.* **2012**, *12*, 5218–5223.

(30) Xu, Z.-Q.; Zhang, Y.; Lin, S.; Zheng, C.; Zhong, Y. L.; Xia, X.; Li, Z.; Sophia, P. J.; Fuhrer, M. S.; Cheng, Y.-B.; Bao, Q. Synthesis and transfer of large-area monolayer WS_2 crystals: moving toward the recyclable use of sapphire substrates. *ACS Nano* **2015**, *9*, 6178–6187.

(31) Polyakov, B.; Kuzmin, A.; Smits, K.; Zideluns, J.; Butanovs, E.; Butikova, J.; Vlassov, S.; Piskunov, S.; Zhukovskii, Y. F. Unexpected epitaxial growth of a few WS_2 layers on {1-100} facets of ZnO nanowires. *J. Phys. Chem. C* **2016**.

(32) Butanovs, E.; Kuzmin, A.; Butikova, J.; Vlassov, S.; Polyakov, B. Synthesis and characterization of ZnO/ZnS/MoS_2 core-shell nanowires. *J. Cryst. Growth* **2017**, *459* (Supplement C), 100–104.

(33) Lan, C.; Li, C.; Wang, S.; Yin, Y.; Guo, H.; Liu, N.; Liu, Y. ZnO–WS_2 heterostructures for enhanced ultra-violet photodetectors. *RSC Adv.* **2016**, *6*, 67520–67524.

(34) R. Dovesi; V. R. Saunders; C. Roetti; R. Orlando; C. M. Zicovich-Wilson; F. Pascale; B. Civalleri; K. Doll; Causà, N. M. H., I. J. Bush, P. D'Arco, M. Llunell, M.; Y. Noël. *CRYSTAL14 User's Manual*; University of Torino: Torino, 2014.

(35) Perdew, J. P.; Ernzerhof, M.; Burke, K. Rationale for mixing exact exchange with density functional approximations. *J. Chem. Phys.* **1996**, *105*, 9982–9985.

(36) Adamo, C.; Barone, V. Toward reliable density functional methods without adjustable parameters: the PBE0 model. *J. Chem. Phys.* **1999**, *110*, 6158–6170.

(37) Evarestov, R. A.; Zhukovskii, Y. F.; Bandura, A. V.; Piskunov, S. Symmetry and models of single-wall BN and TiO_2 nanotubes with hexagonal morphology. *J. Phys. Chem. C* **2010**, *114*, 21061–21069.

(38) Monkhorst, H. J.; Pack, J. D. Special points for Brillouin-zone integrations. *Phys. Rev. B* **1976**, *13*, 5188–5192.

(39) Doebelin, N.; Kleeberg, R. Profex: A graphical user interface for the Rietveld refinement program BGMN. *J. Appl. Crystallogr.* **2015**, *48*, 1573–1580.

(40) Sourisseau, C.; Cruege, F.; Fouassier, M.; Alba, M. Second-order Raman effects, inelastic neutron scattering and lattice dynamics in 2H-WS_2. *Chem. Phys.* **1991**, *150*, 281–293.

(41) Berkdemir, A.; Gutiérrez, H. R.; Botello-Méndez, A. R.; Perea-López, N.; Elías, A. L.; Chia, C.-I.; Wang, B.; Crespi, V. H.; López-Urías, F.; Charlier, J.-C.; Terrones, H; Terrones, M. Identification of individual and few layers of WS_2 using Raman spectroscopy. *Sci. Rep.* **2013**, *3*, 1755.

(42) Liang, L.; Meunier, V. First-principles Raman spectra of MoS_2, WS_2 and their heterostructures. *Nanoscale* **2014**, *6*, 5394–5401.

(43) Mitioglu, A. A.; Plochocka, P.; Deligeorgis, G.; Anghel, S.; Kulyuk, L.; Maude, D. K. Second-order resonant Raman scattering in single-layer tungsten disulfide WS_2. *Phys. Rev. B* **2014**, *89*, 245442.

(44) Lao, C. S.; Liu, J.; Gao, P.; Zhang, L.; Davidovic, D.; Tummala, R.; Wang, Z. L. ZnO nanobelt/nanowire Schottky diodes formed by dielectrophoresis alignment across au electrodes. *Nano Lett.* **2006**, *6*, 263–266.

(45) Perea-López, N.; Elías, A. L.; Berkdemir, A.; Castro-Beltran, A.; Gutiérrez, H. R.; Feng, S.; Lv, R.; Hayashi, T.; López-Urías, F.; Ghosh, S.; et al. Photosensor device based on few-layered WS_2 films. *Adv. Funct. Mater.* **2013**, *23*, 5511–5517.

(46) Huo, N.; Yang, S.; Wei, Z.; Li, S.-S.; Xia, J.-B.; Li, J. Photoresponsive and gas sensing field-effect transistors based on multilayer WS_2 nanoflakes. *Sci. Rep.* **2014**, *4*, 5209.

(47) Carreon, M. L.; Thapa, A. K.; Jasinski, J. B.; Sunkara, M. K. The capacity and durability of amorphous silicon nanotube thin film anode for lithium ion battery applications. *ECS Electrochem. Lett.* **2015**, *4*, A124–A128.

(48) Liu, J.; Li, Y.; Fan, H.; Zhu, Z.; Jiang, J.; Ding, R.; Hu, Y.; Huang, X. Iron oxide-based nanotube arrays derived from sacrificial template-accelerated hydrolysis: large-area design and reversible lithium storage. *Chem. Mater.* **2010**, *22*, 212–217.

(49) Yan, C.; Liu, J.; Liu, F.; Wu, J.; Gao, K.; Xue, D. Tube formation in nanoscale materials. *Nanoscale Res. Lett.* **2008**, *3*, 473–480.

E. Butanovs, S. Vlassov, A. Kuzmin, S. Piskunov, J. Butikova, B. Polyakov,
Fast-response single-nanowire photodetector based on ZnO/WS2 core/shell heterostructures,
ACS Appl. Mater. Interfaces 10 (2018) 13869-13876.

Table of Contents

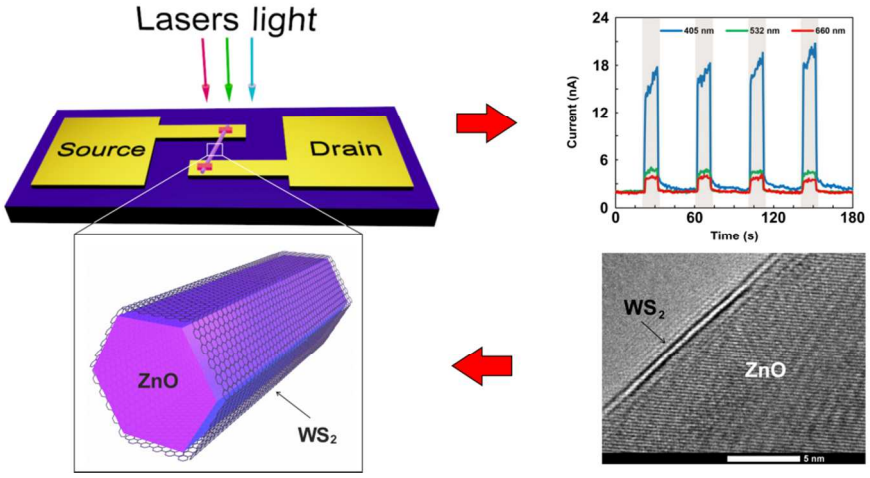

Institute of Solid State Physics, University of Latvia as the Center of Excellence has received funding from the European Union's Horizon 2020 Framework Programme H2020-WIDESPREAD-01-2016-2017-TeamingPhase2 under grant agreement No. 739508, project CAMART²